arXiv:1403.3507v1 [cond-mat.supr-con] 14 Mar 2014

Superconducting tantalum nitride-based normal metal-insulator-superconductor tunnel junctions

S. Chaudhuri[1] and I. J. Maasilta[1,*]

[1] *Nanoscience Center, Department of Physics, University of Jyväskylä, P. O. Box 35, FIN-40014 University of Jyväskylä, Finland*

(Dated: February 28, 2022)

We report the development of superconducting tantalum nitride (TaN_x) normal metal-insulator-superconductor (NIS) tunnel junctions. For the insulating barrier, we used both AlO_x and TaO_x (Cu-AlO_x-Al-TaN_x and Cu-TaO_x-TaN_x), with both devices exhibiting temperature dependent current-voltage characteristics which follow the simple one-particle tunneling model. The superconducting gap follows a BCS type temperature dependence, rendering these devices suitable for sensitive thermometry and bolometry from the superconducting transition temperature T_C of the TaN_x film at ~ 5 K down to ~ 0.5 K. Numerical simulations were also performed to predict how junction parameters should be tuned to achieve electronic cooling at temperatures above 1 K.

Normal metal-insulator-superconductor (NIS) tunnel junction devices aimed at low temperature thermometry, bolometry and refrigeration have witnessed significant developments in the last decade[1,2]. Aluminum (Al) based NIS devices already offer sensitive thermometry in the sub 1 K range[3], and significant cooling power approaching 1 nW at ~ 0.3 K has recently been demonstrated[4,5]. In addition to direct electronic cooling, sizeable indirect phonon cooling of suspended membranes[6–8], beams[9], and a general-purpose refrigeration platform[4] have been achieved using Al coolers. However, to achieve operation at higher temperatures, one must switch to materials with higher superconducting transition temperatures (T_C) than the T_C of Al at ~ 1.2 K, as T_C limits the maximum range of thermometry, and cooling power drops strongly above $T \sim 0.4T_C$[1].

Recently, we fabricated Nb ($T_C \sim 8$ K)[10] and NbN_x ($T_C \sim 12$ K)[11] based NIS devices and demonstrated an order of magnitude increase of the thermometry range, and an observation of some electronic cooling in the Nb device[10]. However, as the optimal operational temperature for cooling for those type of devices is aroung 3.5 - 5 K, one should also develop NIS devices with a T_C in the intermediate range between Al and Nb/NbN devices. This is important because the cooling power also deteriorates fast when the operational temperature is lower than the optimal, and thus Nb or NbN based coolers may not be able to work effectively enough in the temperature range 1 - 3 K. Here, we experimentally demonstrate that tantalum nitride (TaN) with a $T_C \sim 5$K can be used as the superconducting electrode in a micron-scale NIS device. The thermometric characteristics were essentially ideal in the temperature range 0.5 - 5 K, and the observed specific tunneling resistance and the broadening of the superconducting density of states were reasonably low, giving us hope of also developing electronic coolers in the temperature range 1 - 3 K in the future. This was elaborated by numerical simulations, which demonstrated that a further lowering of the specific tunneling resistance of the junctions (in principle a straightforward process) would lead to a sizeable electronic cooling at temperatures around 1.5 - 3 K, despite the observed broadening of the superconducting density of states being higher than for typical Al junctions. In addition, if the broadening could be reduced to levels commonly seen for Al, a truly wonderful device capable of reducing temperature from 1.2 K to 0.2 K would follow.

Tantalum nitride (TaN_x) is a material whose T_C has been shown to be tunable in thin films between 4 - 10.8 K by adjusting the growth parameters[12–15]. Moreover, depending upon the amount of incorporated nitrogen x, TaN_x can be a superconductor, insulator or a metal at low temperatures[12,16,17]. In superconducting device applications, however, TaN has not been used widely. In its normal state, it has been used as a barrier material in SNS Josephson junctions with NbN[18–20] and NbTiN[21] as the superconducting electrode materials. As a superconductor, the only device application so far has been for superconducting single photon detection[22], and notably, no tunnel junction devices have been reported before. Recently, we were able to grow high quality TaN_x thin films with T_C up to ~ 8 K using a pulsed laser deposition (PLD) technique[13]. Furthermore, we have already fabricated NbN_x based NIS junctions, using PLD for the growth of NbN_x films, and electron beam lithography (EBL), reactive ion etching (RIE), and shadow angle evaporation for the device fabrication, with an ex-situ thermally oxidized Al barrier[11]. These two advances were combined here to develop Cu-AlO_x-Al-TaN_x NIS tunnel junctions.

First, 30 nm thick superconducting TaN_x films with T_C in the range ~ 4.5 - 5 K were deposited on (100) oriented MgO single crystals using a PLD technique described in detail elsewhere[13]. A typical temperature dependence of the resistance of such a bare TaN_x film is shown in figure 1(a). MgO was chosen as the substrate, because the films grown on it were shown to be monophase superconducting FCC (rocksalt), while in the films grown on oxidized silicon a coexisting non-superconducting hexagonal phase was also found[13].

The TaN_x films were patterned into 1 μm wide electrodes and large contact pads by electron beam lithog-

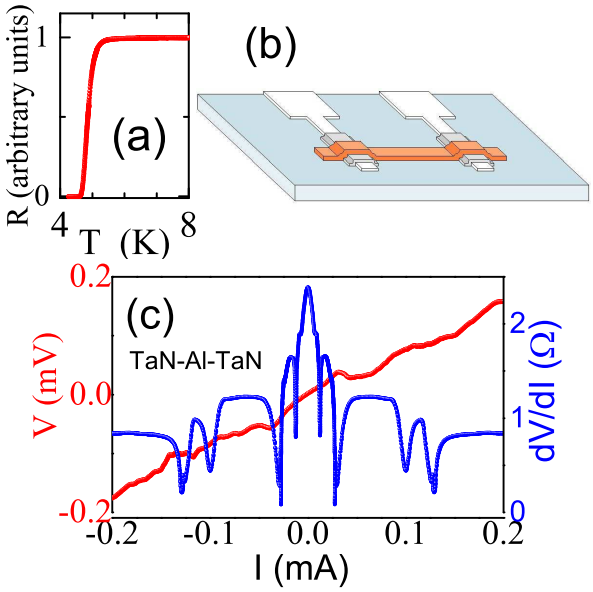


FIG. 1. (Color online) Temperature dependence of the resistance of the bare TaN_x film, used for fabricating the TaN_x-Al-AlO_x-Cu device, exhibiting superconducting transition at ~ 5 K. The ac bias current used was 10 μA. (b) A schematic of a fabricated device with two junctions. Blue: MgO substrate, White: TaN electrodes, Grey: Al/AlOx film, Orange: Cu wire. (c) Bias current dependence of the voltage and differential resistance of a TaN_x-Al-TaN_x SNS junction at 4.2 K.

raphy (EBL) and reactive ion etching (RIE). To make a more resistant etch mask, the TaN_x was first covered with a 50 nm thick evaporated Cu film, on top of which a 400 nm thick positive PMMA resist was spun, followed by EBL electrode patterning and removal of the Cu in the exposed regions with a chemical etch (30 % H_2O_2, glacial acetic acid, DI water 1:1:18). After that, the exposed TaN_x was etched by RIE using CHF_3, 50 sccm and O_2, 5 sccm at a power 100 W and pressure 55 mTorr, the PMMA removed, and finally the remaining Cu removed by another chemical etch step.

The electrode patterning was followed by the fabrication of three distinct types of devices using a second overlay EBL step and ultra-high vacuum (UHV) e-beam evaporation. For the first device type, a 40 nm thick, 0.5 μm wide and 15 μm long aluminum cross strip was deposited across the electrodes, without any explicit attempt to form tunnel barriers. The purpose of this sample is to determine the quality of the Al-TaN_x contact, as an unwanted native oxide barrier may exist on the surface of the TaN_x film. For the second device type, the method previously developed for the NbN_x NIS junction fabrication with AlO_x tunnel barriers has been used[11]. First, 40 nm thick Al islands of size 6 μm$\times$ 6 μm were evaporated on top the TaN_x electrodes, followed by *in-situ* oxidation at room temperature in 50 mbar of O_2 for 4 min, to grow the AlO_x tunnel barriers. Then, without breaking the vacuum, a 100 nm thick Cu strip of width 0.5 μm was evaporated to form the connection between two TaN_x electrodes (separated by a distance of 15 μm) so that a series connection of two Cu-AlO_x-Al-TaN_x NIS tunnel junctions (SINIS) is formed [Fig 1 (b)]. The third device type was identical with the second, except that no Al was deposited, and the TaN_x electrodes were directly oxidized in 400 mbar of O_2 for 30 min. The goal of this process is a SINIS device with a Cu-TaO_x-TaN_x tunnel junction structure. The typical junction dimensions were $\sim 1 \times 0.5$ μm^2.

Since the TaN_x films come in contact with ambient atmosphere for prolonged periods of time during the process of fabrication, we investigated the effects of a possible native oxide barrier with the help of the first type of TaN_x-Al-TaN_x device. The measured voltage and differental resistance vs. current characteristics at 4.2 K are shown figure 1(c). Clearly, the data shows that the contact resistance is low $< 1\Omega$/junction (four orders of magnitude less than the tunneling resistances of the second and third type devices, as will be shown later), and that the general behavior is that of a good NS contact, although several resonance features are seen, possibly originating from multiple Andreev reflections[23]. The resonance features were not observed in similar devices using NbN electrodes[11], however, the NS contact resistance in NbN devices was actually orders of magnitude higher for unknown reasons.

The current-voltage and conductance-voltage measurements for the second and third type devices were carried out using a He^3-He^4 dilution refrigerator. The measurement lines had three stages of filtering: pi-filters at 4.2 K, RC-filters at the base temperature, and microwave filtering[24] between these two (Thermocoax cables of length 1.5 m). For the measurement of conductance, a lock-in technique with a 0.04 mV excitation voltage and 17 Hz frequency was used. In figure 2, the current-voltage ($I-V$) characteristics at various bath temperatures $T_{\rm Bath}$ for a TaN_x-Al-AlO_x-Cu based *double* junction SINIS device are shown in (a) log-linear and (b) linear scales, respectively, together with the corresponding theoretical fits based on the single-particle tunneling model $\frac{1}{eR_T}\int_{-\infty}^{\infty} d\epsilon N_S(\epsilon)(f_N(\epsilon - eV) - f_N(\epsilon + eV))$, where $f_N(\epsilon)$ is the Fermi function in Cu wire, and $N_S(\epsilon)$ is the normalized broadened superconducting quasiparticle density of states (DOS) in the Dynes model[1,25] $N_S(\epsilon, T_S) = \left|{\rm Re}\left(\frac{\epsilon + i\Gamma}{\sqrt{(\epsilon+i\Gamma)^2 - \Delta^2}}\right)\right|$, where Γ is the parameter describing broadening and Δ is the superconducting gap. The corresponding conductance characteristics along with the theoretical fits are shown in figure 2 (c). For all these fits both the superconductor and normal metal temperatures T_S and T_N were set equal to $T_{\rm Bath}$. The dashed lines (most clearly visible for the lowest temperature data in (a) and (c)) assume that the tunneling resistances of the individual junctions are identical, while the solid lines assume non-identical tunneling resistances[26] with proportions 66 % and 34 % of the total resistance. This asymmetry was directly measured

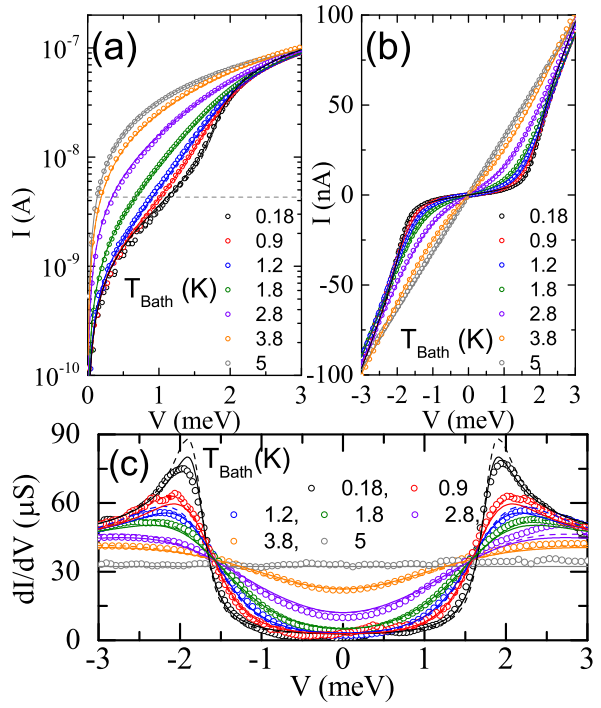


FIG. 2. (Color online) Temperature dependence of the current-voltage characteristics of a double junction based Cu-AlO_x-Al-TaN_x device at various $T_{\rm Bath}$ plotted in (a) log-linear and (b) linear scale. (c) Differential conductance characteristics corresponding to plots in (a). The open symbols denote the measured response, while the lines are the corresponding theoretical fits. The dashed and solid lines corresponds to calculations where the tunnelling resistance of individual junctions are assumed to be equal and unequal (proportions 66 % and 34 %), respectively. The fitting parameters were $\Gamma/\Delta(0) = 7\times10^{-2}$ and $R_{\rm T}$. The horizontal dashed line in (a) represents a constant current bias of 4.3 nA.

with the help of a third NIS junction connected to the same normal metal electrode. The individual junction resistances can then be solved from the three measurements of the SINIS pairs. The agreement between the data and the simplest possible theory with two identical barriers is already very good at higher temperatures, where the effect of the asymmetry is weaker. However, at 0.18 K, the symmetric model predicts a lower sub-gap current (visible at $V \sim 1.5$ mV) than what is observed, and the non-symmetric theory can explain this increase. It is quite important to take into account the asymmetry at low T: Simply fitting to the subgap conductance with T_N as a free parameter would give $T_N \sim 0.5$ K. Such a high electronic overheating is unphysical, as it would require an excess heating power > 100 pW (much higher than$\sim$ 10 fW typically seen in our setup[9]), as estimated from the known electron-phonon interaction constant for Cu[27] and the size of the normal metal island. The physical mechanism for the observed variability in $R_{\rm T}$ is unclear, although it has been suggested[28] that it could result from grain-to-grain barrier variability.

From the fits, we also get the temperature dependence of the superconducting gap Δ, which was seen to follow the simple BCS theory well, in contrast to the NbN_x based devices[11] which exhibited stronger modifications due to proximity effect[29]. At 0.18 K, the measured Δ was $\sim$ 0.9 meV, about four times higher than a typical Al film gap, indicating that the Al layer is well proximized by the TaN_x. This value of Δ is almost the same as in the NbN NIS devices[11] although $T_{\rm C} = 5$ K is less than half, an observation which is consistent with the fact that the contact resistance between TaN_x and Al is much lower. All the theory fits to the $I-V$ and conductance curves were obtained with a broadening parameter $\Gamma/\Delta(0) = 7\times10^{-2}$ [$\Delta(0) = \Delta(T=0)$], a value which is slightly higher than the smallest value observed in the NbN_x devices, $\Gamma_{\rm NbN}/\Delta_{\rm NbN} = 2.4\times10^{-2}$. Similar to the NbN case, strong coupling theory did not fit the data well (not shown). Finally, the total $R_{\rm T}$ of this device was, surprisingly, found to evolve with temperature, from $\sim$ 31 kΩ at 5 K to $\sim$ 26.5 kΩ at 3.8 K and $\sim$ 24.5 kΩ at still lower temperatures. This translates to a specific junction resistance $r_{\rm S}$ of $\sim$ 6.5 k$\Omega\mu$m^2, which is about two orders of magnitude smaller than that in the NbN_x devices fabricated in a similar manner, but still about three-ten times higher than that of typical high power Cu-AlO_x-Al tunnel junction coolers[4,5].

For the devices of the third type (TaN_x-TaO_x-Cu), the yield was quite low - most of them were shorts. However, some were tunnel junctions. In figure 3 (a) and (b), the current-voltage ($I-V$) characteristics at various $T_{\rm Bath}$ of such a TaN_x-TaO_x-Cu *single* NIS junction are shown in (a) log-linear and (b) linear scale, respectively, together with the corresponding theoretical fits. The measured and theoretical conductance curves are shown in figure 3(c). From the theoretical fits the obtained value of $\Gamma/\Delta(0)$ and $\Delta(0)$ were 0.13 and 0.87 meV respectively, with $T_{\rm C} = 4.5$ K being the measured value of the TaN_x film. Here, the obtained value of $R_{\rm T}$ evolved with temperature even more strongly, from $\sim$24 kΩ at 5 K to $\sim$ 16.5 kΩ below 5 K. The origin of this temperature dependence of $R_{\rm T}$ is unclear to us at the moment. The largest change seems to be correlated with the transition to the superconducting state, but some temperature dependence seems to be left even at temperatures much below $T_{\rm C}$. Although the Δ values of TaN_x-TaO_x-Cu and TaN_x-Al-AlO_x-Cu junctions are almost identical, the low yield and the larger value of Γ of the latter render them unfit for real device applications.

Figure 4 shows the thermometric response in the usual measurement configuration where the NIS junction device is current biased, and its voltage (V) response is measured as a function of $T_{\rm Bath}$, of the (a) double junction TaN_x-Al-AlO_x-Cu device and (b) single junction TaN_x-TaO_x-Cu device. For both devices the measured temperature sensitivity was $\sim$ 0.14 mV/K/junction from $T_{\rm C}$ down to $\sim$ 0.5 K, as expected from theory, but at the lowest temperatures there is a saturation and even a curious downturn of the voltage. This downturn cannot

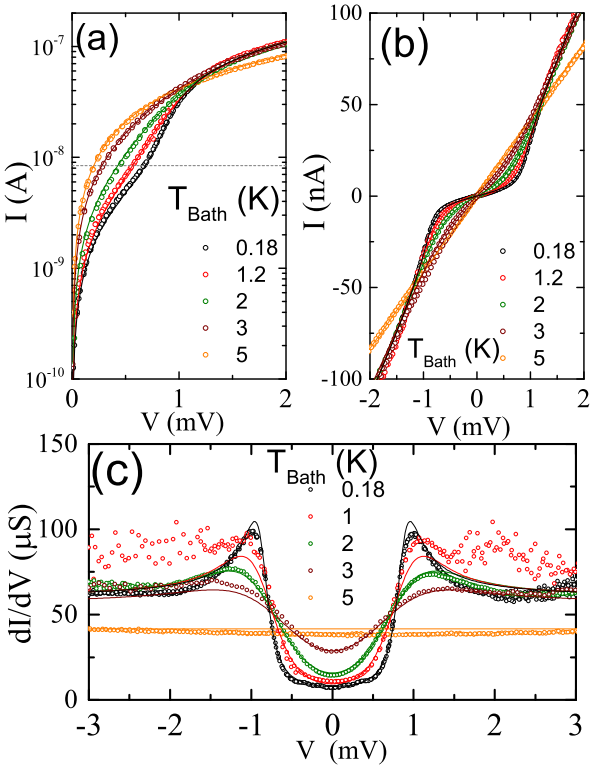


FIG. 3. (Color online) Temperature dependence of the current-voltage characteristics of a single junction based Cu-TaO_x-TaN_x device at various $T_{\rm Bath}$ plotted in (a) log and (b) linear scale. (c) Differential conductance characteristics corresponding to plots in (a). The dots are the experimental data while the solid lines are the corresponding theoretical fits. The fitting parameters were $\Gamma/\Delta(0)$ =0.13 and $R_{\rm T}$. The horizontal dashed line in (a) represents a constant current bias of 8.4 nA.

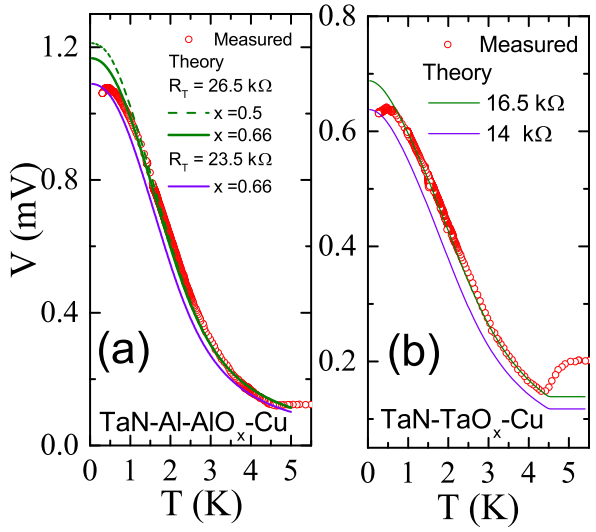


FIG. 4. (Color online) Thermometry characteristics of the (a) Cu-AlO_x-Al-TaN_x junction pair biased with a constant current of $\sim$ 4.3 nA and (b) a single Cu-TaO_x-TaN_x junction biased with $\sim$ 8.4 nA. The dots are the experimental data while the lines indicate the corresponding theoretical fits, assuming a simple one particle tunnelling model with BCS temperature dependence of the superconducting gap, for various cases of $R_{\rm T}$. In (a), dashed line, symmetric $R_{\rm T}$ = 26.5 kΩ, solid green line, asymmetric $R_{\rm T}$ = 26.5 kΩ with with proportions 66 % and 34 % of the two junction resistances, solid purple line, $R_{\rm T}$ = 23.5 kΩ, same asymmetry. In (b), solid green line, $R_{\rm T}$ = 16.5 kΩ, solid purple line, $R_{\rm T}$ = 14 kΩ.

Junction	$\frac{\Gamma}{\Delta(0)}$	$r_{\rm S}$ (kΩμm^2)	$\Delta(0)$ (meV)	$T_{\rm C}$ (K)	Ref.
Al-AlO_x-Cu	1-5×10^{-4}	1-2	0.21	1.4	[9]
Nb-Al-AlO_x-Cu	5×10^{-2}	10	1.0	6	[10]
NbN_x-Al-AlO_x-Cu	2-4×10^{-2}	630-770	1.1	10.8	[11]
NbN_x-NbO_x-Cu	0.2	40	1.1	10.8	[11]
TaN_x-Al-AlO_x-Cu	7×10^{-2}	6.5	0.9	5	
TaN_x-TaO_x-Cu	0.13	8	0.9	4.5	

TABLE I. Broadening of the density of states $\Gamma/\Delta(0)$, specific tunneling resistance $r_{\rm S}$, energy gap at low temperature $\Delta(0)$ and critical temperature $T_{\rm C}$ for various types of junctions. All these junctions were oxidized in the same physical chamber under fairly identical oxidation conditions.

be explained by any theory where $R_{\rm T}$ is temperature independent for such low bias (sub-gap) values[26], and thus the thermometry data confirms the picture of changing $R_{\rm T}$, as can be seen from the representative theory curves.

Having obtained the values for Γ and $r_{\rm S}$ for the TaN NIS devices, we should compare them with previous results using other superconductors. In table I, we have complied results from our lab, fabricated in the same chamber and with fairly similar oxidation parameters. The parameters for TaN_x-Al-AlO_x-Cu junctions seem to be comparable to the earlier results for Nb-Al-AlO_x-Cu junctions. The biggest difference to the standard Al-AlO_x-Cu junction technology is the much larger value of the broadening parameter Γ. The NbN junctions do not seem as promising for cooling as TaN junctions due to the high specific junctions resistances. The DOS broadening seen in our Al-AlO_x-Cu junctions is comparable to the results by other labs[28,30,31]. However, if extreme measures are taken to reduce environmental radiation coupling to the junction, much lower broadening has been demonstrated in Al-AlO_x-Cu junctions[30,32], explained by photon-assisted tunneling. According to that picture $\Gamma/\Delta \sim 1/\Delta$, which suggests that the broadening in our higher gap junctions (Nb,NbN,TaN) is due to some other mechanism.

Finally, to answer better whether TaN based NIS junctions hold promise for cooling applications, we also carried out some numerical simulations. To give an example, all calculations assumed a SINIS device with $T_{\rm C}$ = 5 K and Δ = 0.9 meV, and a Cu normal metal island of thickness 30 nm, with a lateral size the same as the total junction area A. Electron-phonon interaction limited heat flow out of the island was also assumed, which is the typical situation for junctions on bulk substrates[2,9], lead-

ing to heat balance $P_{cool} = \Sigma\Omega(T_{\rm bath}^5 - T_N^5)$, where P_{cool} is the cooling power of the junctions that can be calculated when junctions parameters are known[2,9], Ω is the normal metal volume, and Σ is the electron-phonon coupling constant. A typical value for $\Sigma = 2{\times}10^9$ W/(m^{3}K^5) in Cu was used[27]. Since $P_{cool} \propto A$ and $\Omega \propto A$, the results shown here are independent of A, and therefore we use the specific junction resistance $r_{\rm S}$ as parameter. In figure 5(a) we show the expected decrease of T_N below $T_{\rm Bath}$, as a function of Γ and $T_{\rm Bath}$ for the value of specific junction resistance observed in the experiment $r_{\rm S}$ = 6.5 k$\Omega\mu$m^2. We find that a bit of cooling is expected at low $T_{\rm Bath} \sim 0.2 - 0.3$ K if $\Gamma/\Delta(0)$ could be lowered to values $< 10^{-3}$. However, at that temperature range Al coolers perform better. On the other hand, if the value of $r_{\rm S}$ is lowered, as shown in Fig. 5(b), but $\Gamma/\Delta(0)$ is fixed at the observed value $7{\times}\ 10^{-2}$, a fair amount of cooling (up to 0.3 K) at high $T_{\rm Bath} \sim$ 2 - 3 K is possible when $r_{\rm S} < 10\Omega\mu$m^2. Even this would fall far short from the ultimate goal to cool the metal island from 1.2 K to 0.3 K. In order to achieve such a large magnitude in cooling, a concomitant reduction in $\Gamma/\Delta(0)$ of these TaN$_x$ devices is also necessary. As shown if Fig. 5(c), if $\Gamma/\Delta(0)$ could be lowered to $1{\times}\ 10^{-4}$ (typical for Al devices), then for $r_{\rm S} < 100\ \Omega\mu$m^2 such a large cooling would be theoretically possible. Interestingly, these kind of values for Γ and $r_{\rm S}$ have been obtained experimentally for Al-AlO$_x$-Cu junctions.

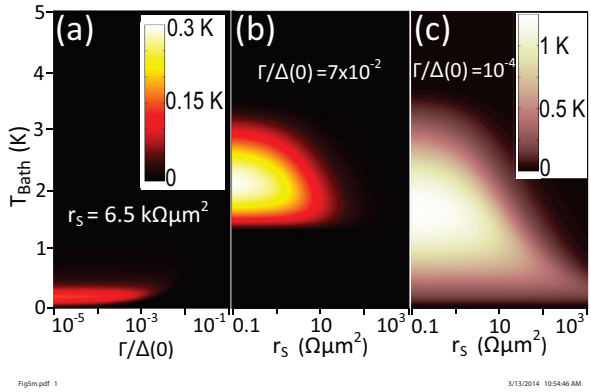


FIG. 5. (Color online) Calculated electronic cooling ($T_{\rm Bath}$ - T_N) for several cases, with electron-phonon limited heat transport and Cu as normal metal. Only regions where net cooling occur ($T_{\rm Bath} \geq T_N$) are shown. (a) Cooling as a function of $T_{\rm Bath}$ and $\Gamma/\Delta(0)$ for r$_S$ = 6.5 k$\Omega\mu$m^2. In (b) and (c), calculated cooling as a function of $T_{\rm Bath}$ and $r_{\rm S}$ for (b) $\Gamma/\Delta(0)$ =$7{\times}\ 10^{-2}$ and (c) $\Gamma/\Delta(0)$ =$1{\times}\ 10^{-4}$. The color bars indicates the magnitude of cooling. The color bar in the inset of (a) serves as the scale for both (a) and (b). It can be seen from (c) that for a device with $\Gamma/\Delta(0) = 1{\times}\ 10^{-4}$ and $r_{\rm S} \sim 10\Omega\mu$m^2, the expected cooling at 1.2 K is $\sim$ 1 K. For all simulations T_C = 5 K and Δ = 0.9 meV.

In conclusion, we have demonstrated the application potential of normal metal-insulator-superconductor tunnel junction devices with TaN as the superconductor. The electrical characteristics of these devices follow the simple one-particle tunneling model, and the superconducting gap exhibit a BCS type temperature dependence. We also demonstrated sensitive thermometry between 0.5 and 5 K, where the lower limit was shown to be caused by an unexpected temperature variability of the tunneling resistance. The measured effective broadening of the superconducting density of states and the specific tunneling resistance of these devices were just high enough to inhibit any electronic cooling. However, as we showed theoretically, a realistic reduction of these parameters for TaN devices would lead to a dramatic breakthrough in the development of practical electronic coolers for 1 K temperature range. Future efforts need to be especially focused on understanding the broadening of the superconducting density of states and how to reduce it.

ACKNOWLEDGEMENTS

This research has been supported by Academy of Finland project number 260880. We thank A. Torgovkin for help with low temperature measurements.

* maasilta@jyu.fi

[1] F. Giazotto, T. T. Heikkilä, A. Luukanen, A. M. Savin, and J. P. Pekola, Rev. Mod. Phys. **78**, 217 (2006).

[2] J. T. Muhonen, M. Meschke, and J. P. Pekola, Rep. Prog. Phys. **75**, 046501 (2012).

[3] M. Nahum and J. M. Martinis, Appl. Phys. Lett. **63**, 3075 (1993).
[4] P. J. Lowell, G. C. O'Neil, J. M. Underwood, and J. N. Ullom, Appl. Phys. Lett. **102**, 082601 (2013).
[5] H. Q. Nguyen, T. Aref, V. J. Kauppila, M. Meschke, C. B. Winkelmann, H. Courtois, and J. P. Pekola, New J. Phys. **15**, 085013 (2013).
[6] A. Luukanen, M. M. Leivo, J. K. Suoknuuti, A. J. Manninen, and J. P. Pekola, J. Low Temp. Phys. **120**, 281 (2000).
[7] A. M. Clark, N. A. Miller, A. Williams, S. T. Ruggiero, G. C. Hilton, L. R. Vale, J. A. Beall, K. D. Irwin, and J. N. Ullom, Appl. Phys. Lett. **86**, 173508 (2005).
[8] N. A. Miller, G. C. O'Neil, J. A. Beall, G. C. Hilton, K. D. Irwin, D. R. Schmidt, L. R. Vale, and J. N. Ullom, Appl. Phys. Lett. **92**, 163501 (2008).
[9] P. J. Koppinen and I. J. Maasilta, Phys. Rev. Lett. **102**, 165502 (2009).
[10] M. R. Nevala, S. Chaudhuri, J. Halkosaari, J. T. Karvonen, and I. J. Maasilta, Appl. Phys. Lett. **101**, 112601 (2012).
[11] S. Chaudhuri, M. R. Nevala, and I. J. Maasilta, Appl. Phys. Lett. **102**, 132601 (2013).
[12] F. M. Kilbane and P. S. Habig, J. Vac. Sci. Technol. **12**, 107 (1975).
[13] S. Chaudhuri, I. J. Maasilta, L. Chandernagor, M. Ging, and M. Lahtinen, J. Vac. Sci. Technol. A **31**, 061502 (2013).
[14] K. Reichelt, W. Nellen, and G. Mair, J. Appl. Phys. **49**, 5284 (1978).
[15] K. Ilin, M. Hofherr, D. Rall, M. Siegel, A. Semenov, A. Engel, K. Inderbitzin, A. Aeschbacher, and A. Schilling, J. Low Temp. Phys. **167**, 809 (2012).
[16] H. Nie, S. Xu, S. Wang, L. You, Z. Yang, C. Ong, J. Li, and T. Liew, Appl. Phys. A **73**, 229 (2001).
[17] L. Yu, C. Stampfl, D. Marshall, T. Eshrich, V. Narayanan, J. M. Rowell, N. Newman, and A. J. Freeman, Phys. Rev. B **65**, 245110 (2002).
[18] A. B. Kaul, S. R. Whiteley, T. Van Duzer, L. Yu, N. Newman, and J. M. Rowell, Appl. Phys. Lett. **78**, 99 (2001).
[19] R. Setzu, E. Baggetta, and J. C. Villegier, J. Phys: Conf. Series **97**, 012077 (2008).
[20] M. Nevala, I. Maasilta, K. Senapati, and R. Budhani, IEEE Trans. Appl. Supercond. **19**, 253 (2009).
[21] L. Yu, R. Gandikota, R. K. Singh, L. Gu, D. J. Smith, X. Meng, T. Zeng, X. Van Duzer, J. M. Rowell, and N. Newman, Supercond. Sci. Technol. **19**, 719 (2006).
[22] A. Engel, A. Aeschbacher, K. Inderbitzin, A. Schilling, K. Ilin, M. Hofherr, M. Siegel, A. Semenov, and H.-W. Hübers, Appl. Phys. Lett. **100**, 062601 (2012).
[23] J. C. Cuevas, J. Hammer, J. Kopu, J. K. Viljas, and M. Eschrig, Phys. Rev. B **73**, 184505 (2006).
[24] A. B. Zorin, Rev. Sci. Instrum. **66**, 4296 (1995).
[25] R. C. Dynes, J. P. Garno, G. B. Hertel, and T. P. Orlando, Phys. Rev. Lett. **53**, 2437 (1984).
[26] S. Chaudhuri and I. J. Maasilta, Phys. Rev. B **85**, 014519 (2012).
[27] J. T. Karvonen, L. J. Taskinen, and I. J. Maasilta, J. Low Temp. Phys. **149**, 121 (2007).
[28] T. Greibe, M. P. V. Stenberg, C. M. Wilson, T. Bauch, V. S. Shumeiko, and P. Delsing, Phys. Rev. Lett. **106**, 097001 (2011).
[29] A. A. Golubov, E. P. Houwman, J. G. Gijsbertsen, V. M. Krasnov, J. Flokstra, H. Rogalla, and M. Y. Kupriyanov, Phys. Rev. B **51**, 1073 (1995).
[30] J. P. Pekola, V. F. Maisi, S. Kafanov, N. Chekurov, A. Kemppinen, Y. A. Pashkin, O.-P. Saira, M. Möttönen, and J. S. Tsai, Phys. Rev. Lett. **105**, 026803 (2010).
[31] G. C. O'Neil, P. J. Lowell, J. M. Underwood, and J. N. Ullom, Phys. Rev. B **85**, 134504 (2012).
[32] O.-P. Saira, A. Kemppinen, V. F. Maisi, and J. P. Pekola, Phys. Rev. B **85**, 012504 (2012).